HHS Public Access

Author manuscript

Chem Mater. Author manuscript; available in PMC 2019 August 09.

Published in final edited form as:

Chem Mater. 2018 February 27; 30(4): 1427–1435. doi:10.1021/acs.chemmater.7b05310.

Mini Gold Nanorods with Tunable Plasmonic Peaks beyond 1000 nm

Huei-Huei Chang[1], **Catherine J. Murphy**[1,*]

Department of Chemistry, University of Illinois at Urbana—Champaign, 600 South Mathews Avenue, Urbana, Illinois 61801, United States

Abstract

Gold nanorods of small sizes have larger absorption cross sections and higher photothermal efficiency compared to larger ones. However, tuning the surface plasmon resonance of small gold nanorods remains a challenge because increasing an aspect ratio usually results from increasing dimensions. We demonstrate the synthesis of mini gold nanorods with tunable longitudinal surface plasmon resonance from ~600 to >1300 nm accompanied by precise control over widths <10 nm. Two weak reducing agents, ascorbic acid and even milder hydroquinone, were applied to a seed-mediated growth method to tune the aspect ratios of mini gold nanorods from 2.2 to 10.8 corresponding to average dimensions 19.3 × 9.0 nm through 93.1 × 8.7 nm, respectively. This seed-mediated growth of mini gold nanorods results in an average 96% of rods and yields of at least 79% based on gold ion reduction. The extinction coefficients of mini gold nanorods were established based on the gold content from inductively coupled plasma mass spectrometry. The longitudinal extinction coefficients range from 1.6×10^8 to 1.4×10^9 M^{-1} cm^{-1} depending on aspect ratio. We show that liter-scale mini gold nanorod syntheses are reproducible, and the dimensions, aspect ratios, and shape percent yields are comparable to those of a small-scale synthesis.

Graphica Abstract

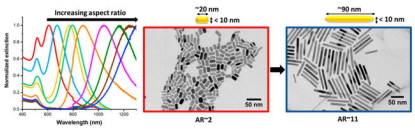

INTRODUCTION

Gold nanoparticles (AuNPs) have been widely used in catalysis,[1–3] sensing,[4,5] imaging,[6–8] and therapeutics[8–10] due to their tunable sizes, tailorable optoelectronic properties, and

*Corresponding Author: murphycj@illinois.edu.

Supporting Information

The Supporting Information is available free of charge on the ACS Publications website at DOI: 10.1021/acs.chemma-ter.7b05310. Additional information about synthesis reagents, mini AuNRs made from different seed-growth solution ratios and from various concentrations of $AgNO_3$ and HCl, single-area electron diffraction data, TEM images, and comparison between mini AuNRs made from 10 and 206 mL seed solutions (PDF)

The authors declare no competing financial interest.

straightforward surface modification.[11–15] Most applications of AuNPs rely on their shape- and size-dependent plasmonic properties. When resonant light impinges upon AuNPs, free electrons oscillate coherently, resulting in localized surface plasmon resonance (LSPR).[16–18] This shape-dependent LSPR allows longitudinal LSPR of gold nanorods (AuNRs) to be tunable from the visible (vis) to the near-infrared (NIR).[16,19–25] The location of the longitudinal LSPR is influenced by particle aspect ratio (AR), which is the length divided by the width of AuNRs. In addition to particle shapes, the plasmonic properties of AuNRs are also size-dependent. The scattering-to-extinction ratio of AuNRs increases with increasing AuNR volume.[24–27] Larger AuNRs are better for scattering-based applications such as imaging and fluorescence enhancement; smaller AuNRs improve photothermal conversion due to higher absorption efficiency.[15,24–28] Fine-tuning of AuNR sizes is warranted to achieve better control over the properties of AuNRs.

Although the LSPR of AuNRs is easily tunable, controlling absolute lengths and widths of AuNRs remains a challenge. The most widely used procedures for AuNR syntheses are seed-mediated methods developed by Nikoobakht and El-Sayed[29] and us.[30] AuNRs made by those methods range from 30 to 80 nm in length and 10 to 20 nm in width.[19,27,31–35] Larger particles have been shown to exhibit slow clearance and low cellular uptake.[36–39] Compared to those standard AuNRs, mini AuNRs (width <10 nm) show better photothermal therapy efficiency, higher cellular uptake, greater tumor accumulation, faster organ clearance, and lower *in vitro* and *in vivo* toxicity.[28,37,40]

Despite sustained interest in mini AuNRs, the challenge of keeping their small sizes, but maintaining tunable plasmonic properties, remains. Mini AuNRs have been synthesized by seedless and seed-mediated growth methods.[28,37,41–44] The seedless method was first reported by Ali et al. in 2012.[41] Four different dimensions of mini AuNRs were formed in *situ* while sodium borohydride ($NaBH_4$) and cetyltrimethylammonium bromide (CTAB) were used as a reducing agent and a surfactant, respectively. The dimensions of those mini AuNRs were tuned by gold, silver nitrate ($AgNO_3$), and $NaBH_4$ concentrations in a growth solution at the optimal pH. The average lengths of those mini AuNRs ranged from 10 to 27 nm, and average widths were all smaller than 5.5 nm. The ARs were from 3.3 to 5.0, and longitudinal LSPR peaks were from 700 to 810 nm. The seedless method was further modified recently by Requejo et al. using poly(vinylpyrrolidone) (PVP) as a shape-directing additive to increase the mini AuNR dimensions to 45 × 6.7 nm corresponding to AR 6.7.[42] In additional to the seedless synthesis, the seed-mediated growth of mini AuNRs was shown by Xu et al. and Jia et al.[2, 44] The longest average length of their mini AuNRs was 45 nm; the available ARs ranged from 2.7 to 4.7, and longitudinal LSPR peaks were tuned from 726 to 829 nm.[28]

Here, we report that the longitudinal LSPR of mini AuNRs can be tuned beyond 1000 nm by the seed-mediated growth method. To achieve better control over LSPR peak positions, we used two reducing agents, ascorbic acid and hydroquinone, to shift the longitudinal LSPR from ~600 to >1300 nm, resulting in mini AuNRs of 9 different ARs (AR 2.2 to AR 10.8). Fine-tuning the ARs was achieved through modifying $AgNO_3$, seed, and hydrochloric acid concentrations in the growth solution. The average widths of mini AuNRs are all less than 10 nm, but the average lengths significantly increase from 19 to 93 nm. Mini AuNR

syntheses result in an average shape yield of 96% in rods, and >79% yield compared to initial gold ion concentrations. The extinction coefficients of mini AuNRs are reported on a per-particle basis. We demonstrate how to scale up mini AuNRs through the synthesis of an extremely large-volume seed solution. Controllable dimensions, ARs, and shape percent yields were shown in both small- and large-scale mini AuNRs.

EXPERIMENTAL SECTION

Materials.

Cetyltrimethylammonium bromide (CTAB, ≥99%), chloroauric acid ($HAuCl_4 \cdot 3H_2O$ ≥ 99.9%), silver nitrate ($AgNO_3$, ≥99%), ascorbic acid (ACS grade), and hydroquinone (≥99%) were purchased from Sigma-Aldrich. Sodium borohydride ($NaBH_4$, ≥99%) was acquired from Fluka. Hydrochloric acid (HCl, certified 1.0 N) and sodium hydroxide (NaOH, 99.0%) were obtained from Fisher Chemical. All chemicals were used as received without further purification.

Synthesis of Ascorbic-Acid-Reduced Mini AuNRs (Aspect Ratio 2.2 ± 0.6 to 3.8 ± 1.0).

A seed solution was prepared according to our previous method.[19] A gold solution was prepared by adding 0.25 mL of 0.010 M $HAuCl_4 \cdot 3H_2O$ to 9.75 mL of 0.10 M CTAB. Ice-cold, freshly prepared 0.60 mL of 0.010 M $NaBH_4$ was quickly added to the stirred gold solution. Immediately, the solution turned from yellow to yellowish brown. After vigorous stirring for 10 min, the solution was kept unstirred at 27 °C for 1.5 h.

To make ascorbic-acid-reduced mini AuNRs, aqueous stock solutions of 0.010 M $AgNO_3$ and 0.10 M ascorbic acid were freshly prepared. All reagents used for mini AuNR syntheses are summarized in Table S1. For a typical 10 mL scale synthesis, mini AuNRs of ARs from ~2.2 to ~3.2 were made by adding 0.50 mL of 0.010 M $HAuCl_4 \cdot 3H_2O$ to 8.0 mL of 0.10 M CTAB. Varied amounts of 0.010 M $AgNO_3$ (from 0.030 to 0.050 to 0.10 mL) were introduced to the growth solutions, and the solutions were gently inverted. In each solution, 0.20 mL of 1.0 M HCl, 80 μL of 0.10 M ascorbic acid, and 2.0 mL of the seed solution were added in sequence, and the growth solutions were inverted in between. Finally, the solutions were set unstirred for 16–20 h at 27 °C and were purified on the next day via centrifugation at 16 000g for 35 min. Colorful supernatant was transferred to a new centrifuge tube and purified by the same centrifugation speed and time again. Pellets were collected and dispersed in nanopure water for further use. Mini AuNRs of AR ~ 3.8 were prepared by the same procedure described above, but with a different growth solution: 9.0 mL of 0.10 M CTAB, 0.10 mL of 0.010 M $AgNO_3$, and 1.0 mL of the seed solution were used. Other solutions were the same as above.

Synthesis of Hydroquinone-Reduced Mini AuNRs (Aspect Ratio 5.6 ± 1.3 to 10.8 ± 2.8).

Seeds for hydroquinone-reduced synthesis were prepared based on procedures developed by Vigderman and Zubarev.[20] A gold solution containing 0.50 mL of 0.010 M $HAuCl_4 \cdot 3H_2O$ and 9.5 mL of 0.10 M CTAB was prepared. Next, ice-cold, freshly prepared 0.46 mL of 0.010 M $NaBH_4$ in 0.010 M of NaOH was quickly added to the stirred gold solution.

Immediately, the solution turned from yellow to brown. After being stirred for 10 min, the solution was kept unstirred at 27 °C for 2 h.

Mini AuNRs of ARs from ~5.6 to ~10.8 were obtained by varying HCl concentrations in growth solutions, but a fixed concentration of $AgNO_3$ was used. Stock solutions 0.10 M $AgNO_3$ and 0.10 M hydroquinone were freshly made. Five 10 mL growth solutions were prepared. Each solution contained 0.50 mL of 0.010 M $HAuCl_4{\cdot}3H_2O$ and 8.0 mL of 0.10 M CTAB. Next, 40 μL of 0.10 M $AgNO_3$ was introduced to each growth solution, and the solution was gently inverted. Increasing amounts of HCl resulted in higher-aspect-ratio mini AuNRs: Various amounts of 1.0 M HCl (0, 13, 19, 25, and 36 μL) were introduced to the growth solutions, and the solutions were gently inverted. Then, 0.50 mL of 0.10 M hydroquinone was added to growth solutions, and the solutions were inverted. Until the solutions turned to completely colorless, 2.0 mL of the seed solution was added. Finally, the solutions were set unstirred for 16–20 h at 27 °C and were purified on the next day via centrifugation at 16 000g for 35 min. The supernatant was removed; the pellet was dispersed in nanopure water.

Large-Scale Mini AuNR Synthesis.

Preparation of a 206 mL Gold Seed Solution.—To scale up mini AuNRs to ~1 L, a seed solution of at least 200 mL is required. First, a solution containing 200 mL and 850 μL of 0.10 M CTAB was prepared. Next, 5.15 mL of 0.010 M $HAuCl_4{\cdot}3H_2O$ was added to the CTAB solution. Quickly, eight 1 mL aliquots and 50 μL of ice-cold, freshly prepared 0.010 M $NaBH_4$ were added to the stirred gold solution with a single channel pipet. The solution turned from yellow to yellowish brown. After vigorous stirring for 10 min, the solution was kept unstirred at 27 °C for 1.5 h.

Synthesis of Large-Scale Mini AuNRs.—A ~1 L mini AuNR growth solution made by ascorbic acid reduction was prepared by directly scaling up all solutions. Reagent concentrations and temperature were kept the same as those of a 10 mL scale synthesis. To make mini AuNRs of AR ~2, 50 mL of 0.010 M $HAuCl_4{\cdot}3H_2O$ was added to 800 mL of 0.10 M CTAB. Next, 3.0 mL of 0.010 M $AgNO_3$ was introduced to the growth solution, and the solution was gently swirled. The following solutions were added in sequence, and the growth solution was swirled in between: 20 mL of 1.0 M HCl, 8.0 mL of 0.10 M ascorbic acid, and 200 mL of the seed solution prepared in the previous paragraph. Finally, the solution was set unstirred for 16–20 h at 27 °C and was purified on the next day via centrifugation at 15 000g for 20 min. The supernatant was removed, and the pellet was redispersed in nanopure water.

Characterization.

UV-vis-NIR spectra were measured with a Cary 5000 UV-vis-NIR spectrophotometer (Agilent Technologies). Transmission electron microscopy (TEM) images of mini AuNRs were collected by a JEOL 2010 LaB6 or a JEOL 2100 Cryo microscope (JEOL Ltd., Tokyo, Japan). Average lengths, widths, ARs, and shape percent yields of mini AuNRs were determined by ImageJ software (the National Institutes of Health). At least 300 particles were counted to determine the dimensions of each batch of mini AuNRs. Inductively

coupled plasma mass spectrometry (ICP-MS) was used to determine the gold concentration of each growth solution. A minimum of three measurements were taken for each batch of mini AuNRs using a Thermo-Finnigan Element XR ICP-MS instrument (Thermo Fisher Scientific).

RESULTS AND DISCUSSION

We report the syntheses of mini AuNRs of different ARs by the seed-mediated approach: A seed solution and a growth solution were prepared to separate nucleation and growth steps (Figure 1). The seed solution used for ascorbic-acid-reduced syntheses was identical to that used for the standard AuNR synthesis. The major differences between mini and standard AuNR syntheses are (i) a dramatic increase in the volume of a seed solution added to the growth solution and (ii) a lower pH of the growth solution.[28] Figure 2a shows the UV-vis-NIR spectra of mini AuNRs from AR 2.2 to 2.6, 3.2, and 3.8. Their maximal longitudinal plasmon band wavelengths are at 607, 673, 741, and 793 nm, respectively. Increasing AR from 2.2 to 3.2 was achieved by increasing $AgNO_3$ concentrations in the growth solutions. This result is consistent with the well-known method of tuning AuNR ARs by $AgNO_3$.[29] However, the increase in ARs from 3.2 to 3.8 did not rely on changes of $AgNO_3$ concentrations, but resulted from a decrease in the volume of a seed solution added to the growth solution. (In both growth solutions, the $AgNO_3$ concentration was fixed at 92 μM, but the ratio of a seed to growth solution was decreased from 1:4 to 1:9.) Figure S1 shows that mini AuNR ARs can be tuned by gradually decreasing a seed-growth solution ratio from 9:1 to 1:9 but with the same $AgNO_3$ concentration. Tuning nanoparticle sizes via controlling the amount of seeds in the growth solution has been demonstrated in both gold nanosphere and rod syntheses.[28,45] Particles grow smaller when there are more seeds in a growth solution. Each seed will receive less Au^0 deposition under the limited amount of Au^{3+} put in the growth solution; conversely, particles become larger when fewer seeds are available in the growth solution.

Table 1 shows the ARs, dimensions, and yields of mini AuNRs made from ascorbic-acid-reduced syntheses. The dimensions, ARs, and shape percent yields were calculated based on TEM images shown in Figure 2b–e. Despite distinct longitudinal plasmon band maxima accompanied by increasing $AgNO_3$ concentrations, the lengths of mini AuNRs are very similar: 19.3 ± 4.8, 19.2 ± 5.3, and 20.5 ± 6.5 nm, which correspond to ARs 2.2, 2.6, and 3.2. The effect of $AgNO_3$ on the anisotropic growth of mini AuNRs seems less influential in lengths; however, widths decrease more obviously from 9.0 ± 1.7 to 6.5 ± 1.3 nm. An inverse correlation is shown between increases in the amount of $AgNO_3$ and decreases in the widths, resulting in increasing ARs. The reduction yields of ascorbic-acid-reduced mini AuNRs are at least 79%, which is significantly higher than ~15% reported from standard AuNRs.[46]

To achieve higher ARs, the weaker reducing agent hydroquinone was used instead of ascorbic acid.[20] Mini AuNRs of AR 5.6–10.8 were prepared by tuning HCl concentrations in the growth solutions under a fixed $AgNO_3$ concentration. The concentration of HCl varied from 0 to 3.3 mM, but the $AgNO_3$ concentration was fixed at 0.36 mM for all growth solutions. Figure 3a shows the normalized extinction spectra of hydroquinone-reduced mini

AuNRs made from different HCl concentrations. Increasing the amounts of HCl in the growth solutions resulted in gradual red-shifts of longitudinal LSPR peaks: the plasmon bands shifted from 875 to 1040, 1167, 1245, and >1300 nm. Figure 3b–e and Table 2 show that the dimensions and ARs of hydroquinone-reduced mini AuNRs increase with increasing the HCl concentration in the growth step. The lengths of hydroquinone-reduced mini AuNRs, unlike ascorbic-acid-reduced ones, increase significantly from 27.2 ± 4.4 to 93.1 ± 18.3 nm. The average widths also increase; however, all are precisely controlled within 10 nm (from 5.0 ± 0.5 to 8.7 ± 1.0 nm). The ARs of hydroquinone-reduced mini AuNRs are tunable by changing the HCl concentration in the growth solutions. The smallest AR is 5.6 obtained with no HCl in the growth solution. The largest AR 10.8 resulted from introducing the highest amount of HCl to the growth solution. These dimensions 93.1 ± 18.3 × 8.7 ± 1.0 nm are unique since reported AuNRs with similar lengths are larger than 20 nm in width.[20,22,23,47] All hydroquinone-reduced mini AuNRs produce high shape percent yields (>95%), and reduction yields are nearly quantitative (~100%).

The HCl concentration in the growth solution is crucial, since the hydroquinone reduction potential is pH-dependent.[48,49] We observed that different HCl concentrations in the growth solutions, indeed, tuned the final AuNR ARs, but a further increase of the HCl concentration (from 3.3 to 4.5 mM) increases neither the lengths, widths, nor ARs of hydroquinone-reduced mini AuNRs. The average lengths and widths of hydroquinone-reduced mini AuNRs made from 3.3 and 4.5 mM of HCl are similar, 93.1 ± 18.2 and 92.6 ± 18.3 nm in length and 8.7 ± 1.0 and 8.7 ± 1.1 nm in width, respectively, and their ARs are the same (Table S3 and Figure S2).

For standard AuNRs, it is well-known that the aspect ratio of the particles is tuned by the concentration of $AgNO_3$: When there is more silver in the growth solution, the aspect ratio is higher.[29,30] The effect of $AgNO_3$ on the ARs of hydroquinone-reduced mini AuNRs was investigated in the absence and presence of HCl. When no HCl was in the growth solutions, hydroquinone-reduced mini AuNRs were not tunable by $AgNO_3$: The maximum wavelengths only shift from 772 to 881 nm despite increases of $AgNO_3$ concentrations from 0.091 to 0.36 mM (Figure S3). No linear relationship between increases in the $AgNO_3$ concentration and the longitudinal plasmon band maximum was found, in contrast to the “standard” synthesis. However, in the presence of HCl, the correlation between the $AgNO_3$ concentration in the growth solution and the position of the longitudinal plasmon band is linear (Figure S4a). Ultimately, longitudinal LSPR peaks showed continual red-shifts from 673 to 989, 1242, and >1300 nm in the presence of 2.3 mM of HCl with increasing $AgNO_3$ concentration. Although the longitudinal LSPR peaks are tunable by varying $AgNO_3$ concentrations, many byproducts appear in the growth solutions when the $AgNO_3$ concentrations were low (Figure S4b,c). The plasmon band tunability of hydroquinone-reduced mini AuNRs relies more on the presence of HCl than $AgNO_3$ in the growth solutions, for reasons that are not yet clear. Possibilities include (i) the pH-dependent reduction potential of hydroquinone, and (ii) the chloride counterion that can form $AgCl_{(s)}$ and $AgCl_2^-$ complex ions under our conditions. Recent work in the literature suggests that silver underpotential deposition on specific crystal facets, mediated by the presence of complexing ions, might be the symmetry-breaking foundation of nanorod formation;[50]

therefore, silver-chloride complexes may require chloride from HCl in addition to chloride from $HAuCl_4$.

Figure 4a shows the linear relationship between ARs of mini AuNRs and the corresponding maximal longitudinal plasmon band wavelengths. The standard deviations in ARs become significantly larger as ARs increase beyond 8.2. We did not include AR 10.8 on Figure 4a because the maximal wavelength is larger than 1300 nm, which is not spectroscopically detectable due to water absorption. The average widths are all less than 10 nm as shown in Figure 4b. The average widths of mini AuNRs decrease as ARs increase from 2.2 to 5.6; the widths, however, increase as ARs increase from 5.6 to 10.8. Figure 4c shows the correlation between increases in the ARs and increases in the lengths of mini AuNRs.

Table 3 shows extinction coefficients of mini AuNRs from AR 2.2 to 10.8, from ICP-MS detection of metal ions from aqua-regia-digested rods in concert, and assuming the bulk face-centered-cubic (fcc) crystal structure of gold with a = 4.08 Å The longitudinal extinction coefficients range from 1.6×10^8 to 1.4×10^9 M^{-1} cm^{-1}. Mini AuNRs of ARs less than 5.6 show 10-fold smaller extinction coefficients (~2×10^8 M^{-1} cm^{-1}) compared to those of standard AuNRs ($2.5–5.5 \times 10^9$ M^{-1} cm^{-1}).[46] The results, are consistent with the extinction coefficient 1.9×10^8 M^{-1} cm^{-1} (AuNRs with dimensions 25 × 5 nm) reported by Ali et al.[40] As the AR increases to 8.2, the extinction coefficient of mini AuNRs increases to 1.4×10^9 M^{-1} cm^{-1}. This magnitude is still smaller than the smallest extinction coefficient of standard AuNRs (2.5×10^9 M^{-1} cm^{-1}) due to the relatively small volume of mini AuNRs.[46] Figure S5 shows single-area electron diffraction data for ascorbic-acid- and hydroquinone-reduced mini AuNRs. Unlike our original penta-twinned rods, the materials are single crystalline.[51] Detailed information about planes and interplanar spacings is available in the Supporting Information.

We achieved mini AuNRs from AR 2.2 to AR 10.8 on a small scale (a 10 mL growth solution). However, the challenge of a large-scale synthesis of mini AuNRs arises from the necessity of a significant increase in seed solution volume. To make 10 mL mini and standard AuNR growth solutions, 2 mL and 12 μL seed solutions are required, respectively. Scaling up mini AuNRs to a 400 mL growth solution thus needs an 80 mL seed solution. This is an enormous amount compared to the 480 μL of seeds to make 400 mL standard AuNRs. Through modifying the concentration of $NaBH_4$, we demonstrate how to make seed solutions up to 206 mL (see the Experimental Section). The ranges of $NaBH_4$ concentrations required to produce acceptable seed solutions from 21 to 206 mL are summarized in Figure S6a. As the volume of a seed solution becomes larger, the acceptable range of $NaBH_4$ concentrations becomes narrower: To make a mini AuNR growth solution that produces >90% shape percent yields, the acceptable $NaBH_4$ concentrations are 0.37–0.41 mM for a 21 mL seed solution, but only 0.376 mM of $NaBH_4$ produces a 206 mL seed solution. Figure S6b,c shows CTAB-capped Au seeds made from 10 mL and 206 mL seed solutions. Their morphology and sizes are similar. Sizes for seeds made from 10 and 206 mL seed solutions are 1.9 ± 0.5 nm (N = 392) and 1.5 ± 0.4 nm (N = 422), respectively. The seeds made from a 10 mL seed solution are slightly larger.

We sought to compare the relative abilities of small- and large-scale seeds to grow monodisperse rods. Below shows the result of ascorbic-acid-reduced mini AuNRs from two 10 mL growth solutions. One growth solution was made from a standard 10 mL seed solution, and the other was synthesized from a 206 mL seed solution. All growth solutions contained 46 μM of $AgNO_3$, aiming for AR ~ 2.6. Figure S8a shows UV-vis-NIR spectra of ascorbic-acid-reduced mini AuNRs made from 10 mL and 206 mL seed solutions. Their maximum wavelengths are similar: The former is at 658 nm and the latter at 650 nm. Figure S7b,c shows the TEM images of mini AuNRs made from 10 and 206 mL seed solutions, respectively. Their lengths, widths, ARs, and shape percent yields are all very comparable as shown in Table S4: 19.2 ± 5.3 and 19.6 ± 4.3 nm in length, 7.6 ± 1.7 and 8.0 ± 1.7 in width, and 2.6 ± 0.7 and 2.5 ± 0.7 in AR. Consistent with the UV-vis-NIR spectra, mini AuNRs made from the 206 mL seed solution show smaller standard deviations of the dimensions and a slightly higher shape percent yield.

It has been shown in the previous section that mini AuNRs made from 10 and 206 mL seed solutions are comparable. With this large amount of the seed solution, a 1 L mini AuNR growth solution should be possible. Each 10 mL growth solution of mini AuNRs requires 2 mL of a seed solution. Therefore, with a 206 mL seed solution, 1.03 L of a mini AuNR growth solution can be made. Also, more than 170 L of a growth solution containing standard AuNRs could be made because each 10 mL growth solution only needs 12 μL of a seed solution. We did not synthesize 170 L of standard rods due to the complexity of making such a large scale in the lab, but we show, below, how to make 1 L batches of mini AuNRs.

Three individual 1 L mini AuNR growth solutions were synthesized to test the reproducibility of large-scale mini AuNRs and were compared to a small-scale synthesis (10 mL growth solutions). To compare the reproducibility of 1 L mini AuNRs, all growth solutions were prepared by the ascorbic-acid-reduced method and contained 28 μM of $AgNO_3$ (aiming for AR ~ 2.2), but made from three individual 206 mL seed solutions on different days. The UV-vis-NIR spectra of those trials are shown in Figure 5a. Figure 5b–d shows the TEM images of mini AuNRs from three 1 L batches. All three batches have widths less than 10 nm and shape percent yields higher than 97% (Table 4). Although there are some slight differences in the maximum wavelengths, ARs, and lengths between batches, the average dimension, AR, and shape percent yields are comparable to mini AuNR of AR 2.2 from a 10 mL synthesis (Table 1). The 1 L batch renders an average concentration of 1.1 × 10^{-7} M of mini AuNRs, which can be further reconstituted to form micromolar concentration sufficient for most biological applications. We demonstrate large-scale mini AuNRs were reproducible with respect to controlling widths less than 10 nm and achieving desired ARs, and high shape percent and reduction yields.

CONCLUSIONS

We demonstrate how to make mini AuNRs with a wide range of ARs from 2.2 to 10.8 by a seed-mediated growth approach. Their longitudinal LSPR can be finely tuned from ~600 to >1300 nm through changes of reducing agents and modifying $AgNO_3$, HCl, and seed concentrations in the growth solution. Despite the lengths of mini AuNRs ranging from 19 to 93 nm, precise control over widths has been shown: All were less than 10 nm. This seed-

mediated growth of mini AuNRs offers high gold ion reduction (>79%) compared to ~15% yield from the standard AuNR synthesis.[45] Scaling up mini AuNRs to 1 L has been achieved through an extremely large-volume seed solution, producing comparable mini AuNRs as the small-scale synthesis. This large-volume seed solution also benefits other AuNR syntheses. We have shown that large-scale synthesis of mini AuNRs is reproducible with the controllable widths and ARs along with high shape percent and reduction yields.

Supplementary Material

Refer to Web version on PubMed Central for supplementary material.

ACKNOWLEDGMENTS

This work is supported by the National Institutes for Health Grant 5R21-HL129115-02. We gratefully acknowledge Dr. Lijian He of the Mass Spectrometry Center at the University of South Carolina for ICP-MS acquisition. We also thank Dr. Wacek Swiech for assistance with electron diffraction. TEM was carried out in the Frederick Seitz Materials Research Laboratory Central Facilities at the University of Illinois.

REFERENCES

(1). Neri S; Martin SG; Pezzato C; Prins LJ Photoswitchable Catalysis by a Nanozyme Mediated by a Lightsensitive Cofactor. J. Am. Chem. Soc 2017, 139, 1794–1797. [PubMed: 28121141]

(2). Zhan W; Shu Y; Sheng Y; Zhu H; Guo Y; Wang L; Guo Y; Zhang J; Lu G; Dai S Surfactant-Assisted Stabilization of Au Colloids on Solids for Heterogeneous Catalysis. Angew. Chem., Int. Ed 2017, 56, 4494–4498.

(3). Dhiman M; Chalke B; Polshettiwar V Organosilane Oxidation with a Half Million Turnover Number Using Fibrous Nanosilica Supported Ultrasmall Nanoparticles and Pseudo-Single Atoms of Gold. J. Mater. Chem. A 2017, 5, 1935–1940.

(4). Chen Y; Xianyu Y; Jiang X Surface Modification of Gold Nanoparticles with Small Molecules for Biochemical Analysis. Acc. Chem. Res 2017, 50, 310–319. [PubMed: 28068053]

(5). Deng C; Pi X; Qian P; Chen X; Wu W; Xiang J High-Performance Ratiometric Electrochemical Method Based on the Combination of Signal Probe and Inner Reference Probe in One Hairpin-Structured DNA. Anal. Chem 2017, 89, 966–973. [PubMed: 27983797]

(6). Kim T; Lee N; Arifin DR; Shats I; Janowski M; Walczak P; Hyeon T; Bulte JWM In Vivo Micro-CT Imaging of Human Mesenchymal Stem Cells Labeled with Gold-Poly-l-Lysine Nano-complexes. Adv. Funct. Mater 2017, 27, 1604213. [PubMed: 28713230]

(7). Shang W; Zeng C; Du Y; Hui H; Liang X; Chi C; Wang K; Wang Z; Tian J Core-Shell Gold Nanorod@Metal-Organic Framework Nanoprobes for Multimodality Diagnosis of Glioma. Adv. Mater 2017, 29, 1604381.

(8). Cheng X; Sun R; Yin L; Chai Z; Shi H; Gao M Light-Triggered Assembly of Gold Nanoparticles for Photothermal Therapy and Photoacoustic Imaging of Tumors In Vivo. Adv. Mater 2017, 29, 1604894.

(9). Her S; Jaffray DA; Allen C Gold Nanoparticles for Applications in Cancer Radiotherapy: Mechanisms and Recent Advancements. Adv. Drug Delivery Rev 2017, 109, 84–101.

(10). Riley RS; Day ES Gold Nanoparticle-Mediated Photothermal Therapy: Applications and Opportunities for Multimodal Cancer Treatment. Wiley Interdiscip. Rev.: Nanomed. Nanobiotechnol 2017, 9, e1449.

(11). Burrows ND; Lin W; Hinman JG; Dennison JM; Vartanian AM; Abadeer NS; Grzincic EM; Jacob LM; Li J; Murphy CJ Surface Chemistry of Gold Nanorods. Langmuir 2016, 32, 9905–9921. [PubMed: 27568788]

(12). Li N; Zhao P; Astruc D Anisotropic Gold Nanoparticles: Synthesis, Properties, Applications, and Toxicity. Angew. Chem., Int. Ed 2014, 53, 1756–1789.

(13). Daniel M-C; Astruc D Gold Nanoparticles: Assembly, Supramolecular Chemistry, Quantum-Size-Related Properties, and Applications Toward Biology, Catalysis, and Nanotechnology. Chem. Rev 2004, 104, 293–346. [PubMed: 14719978]

(14). Dreaden EC; Alkilany AM; Huang X; Murphy CJ; El-Sayed MA The Golden Age: Gold Nanoparticles for Biomedicine. Chem. Soc. Rev 2012, 41, 2740–2779. [PubMed: 22109657]

(15). Huang X; Neretina S; El-Sayed MA Gold Nanorods: From Synthesis and Properties to Biological and Biomedical Applications. Adv. Mater 2009, 21, 4880–4910. [PubMed: 25378252]

(16). Lohse SE; Murphy CJ The Quest for Shape Control: A History of Gold Nanorod Synthesis. Chem. Mater 2013, 25, 12501261.

(17). Willets KA; Van Duyne RP Localized Surface Plasmon Resonance Spectroscopy and Sensing. Annu. Rev. Phys. Chem 2007, 58, 267–297. [PubMed: 17067281]

(18). Talapin DV; Lee J-S; Kovalenko MV; Shevchenko EV Prospects of Colloidal Nanocrystals for Electronic and Optoelectronic Applications. Chem. Rev 2010, 110, 389–458. [PubMed: 19958036]

(19). Abadeer NS; Brennan MR; Wilson WL; Murphy CJ Distance and Plasmon Wavelength Dependent Fluorescence of Molecules Bound to Silica-Coated Gold Nanorods. ACS Nano 2014, 8, 8392–8406. [PubMed: 25062430]

(20). Vigderman L; Zubarev ER High-Yield Synthesis of Gold Nanorods with Longitudinal SPR Peak Greater than 1200 nm Using Hydroquinone as a Reducing Agent. Chem. Mater 2013, 25, 14501457.

(21). Ye X; Jin L; Caglayan H; Chen J; Xing G; Zheng C; Doan-Nguyen V; Kang Y; Engheta N; Kagan CR; Murray CB Improved Size-Tunable Synthesis of Monodisperse Gold Nanorods through the Use of Aromatic Additives. ACS Nano 2012, 6,2804–2817. [PubMed: 22376005]

(22). Ye X; Zheng C; Chen J; Gao Y; Murray CB Using Binary Surfactant Mixtures to Simultaneously Improve the Dimensional Tunability and Monodispersity in the Seeded Growth of Gold Nanorods. Nano Lett. 2013, 13, 765–771. [PubMed: 23286198]

(23). Zhang L; Xia K; Lu Z; Li G; Chen J; Deng Y; Li S; Zhou F; He N Efficient and Facile Synthesis of Gold Nanorods with Finely Tunable Plasmonic Peaks from Visible to Near-IR Range. Chem. Mater 2014, 26, 1794–1798.

(24). Link S; El-Sayed MA Spectral Properties and Relaxation Dynamics of Surface Plasmon Electronic Oscillations in Gold and Silver Nanodots and Nanorods. J. Phys. Chem. B 1999, 103, 8410–8426.

(25). Lai J; Zhang L; Niu W; Qi W; Zhao J; Liu Z; Zhang W; Xu G One-Pot Synthesis of Gold Nanorods Using Binary Surfactant Systems with Improved Monodispersity, Dimensional Tunability and Plasmon Resonance Scattering Properties. Nanotechnology 2014, 25, 125601. [PubMed: 24571958]

(26). Park K; Biswas S; Kanel S; Nepal D; Vaia RA Engineering the Optical Properties of Gold Nanorods: Independent Tuning of Surface Plasmon Energy, Extinction Coefficient, and Scattering Cross Section. J. Phys. Chem. C 2014, 118, 5918–5926.

(27). Ni WH; Kou XS; Yang Z; Wang J Longitudinal Surface Plasmon Wavelengths, Scattering and Absorption Cross Sections of Gold Nanorods. ACS Nano 2008, 2 (4), 677–686. [PubMed: 19206598]

(28). Jia H; Fang C; Zhu X-M; Ruan Q; Wang Y-XJ; Wang J Synthesis of Absorption-Dominant Small Gold Nanorods and Their Plasmonic Properties. Langmuir 2015, 31, 7418–7426. [PubMed: 26079391]

(29). Nikoobakht B; El-Sayed MA Preparation and Growth Mechanism of Gold Nanorods (NRs) Using Seed-Mediated Growth Method. Chem. Mater 2003, 15, 1957–1962.

(30). Sau TK; Murphy CJ Seeded High Yield Synthesis of Short Au Nanorods in Aqueous Solution. Langmuir 2004, 20, 6414–6420. [PubMed: 15248731]

(31). Burrows ND; Harvey S; Idesis FA; Murphy CJ Understanding the Seed-Mediated Growth of Gold Nanorods through a Fractional Factorial Design of Experiments. Langmuir 2017, 33, 1891–1906. [PubMed: 27983861]

(32). Liao H; Hafner JH Gold Nanorod Bioconjugates. Chem.Mater 2005, 17, 4636–4641.

(33). Wu J; Xu Y; Li D; Ma X; Tian H End-to-End Assembly and Disassembly of Gold Nanorods based on Photo-Responsive Host-Guest Interaction. Chem. Commun 2017, 53, 4577–4580.

(34). Dickerson EB; Dreaden EC; Huang X; El-Sayed IH; Chu H; Pushpanketh S; McDonald JF; El-Sayed MA Gold Nanorod Assisted Near-Infrared Plasmonic Photothermal Therapy (PPTT) of Squamous Cell Carcinoma in Mice. Cancer Lett. 2008, 269, 57–66. [PubMed: 18541363]

(35). Wang H; Huff TB; Zweifel DA; He W; Low PS; Wei A; Cheng J-X In Vitro and in Vivo Two-Photon Luminescence Imaging of Single Gold Nanorods. Proc. Natl. Acad. Sci U. S. A 2005, 102, 1575215756.

(36). Jiang W; Kim BYS; Rutka JT; Chan WCW Nanoparticle-Mediated Cellular Response Is Size-Dependent. Nat. Nanotechnol 2008, 3, 145–150. [PubMed: 18654486]

(37). Li Z; Tang S; Wang B; Li Y; Huang H; Wang H; Li P; Li C; Chu PK; Yu X-F Metabolizable Small Gold Nanorods: Size-Dependent Cytotoxicity, Cell Uptake and in Vivo Biodistribution. ACS Biomater. Sci. Eng 2016, 2, 789–797.

(38). Cheng X; Tian X; Wu A; Li J; Tian J; Chong Y; Chai Z; Zhao Y; Chen C; Ge C Protein Corona Influences Cellular Uptake of Gold Nanoparticles by Phagocytic and Nonphagocytic Cells in a Size-Dependent Manner. ACS Appl. Mater. Interfaces 2015, 7,20568–20575. [PubMed: 26364560]

(39). Oh N; Park J-H Surface Chemistry of Gold Nanoparticles Mediates Their Exocytosis in Macrophages. ACS Nano 2014, 8, 62326241.

(40). Song J; Yang X; Jacobson O; Huang P; Sun X; Lin L; Yan X; Niu G; Ma Q; Chen X Ultrasmall Gold Nanorod Vesicles with Enhanced Tumor Accumulation and Fast Excretion from the Body for Cancer Therapy. Adv. Mater 2015, 27, 4910–4917. [PubMed: 26198622]

(41). Ali MRK; Snyder B; El-Sayed MA Synthesis and Optical Properties of Small Au Nanorods using a Seedless Growth Technique. Langmuir 2012, 28, 9807–9815. [PubMed: 22620850]

(42). Requejo KI; Liopo AV; Derry PJ; Zubarev ER Accelerating Gold Nanorod Synthesis with Nanomolar Concentrations of Poly(vinylpyrrolidone). Langmuir 2017, 33, 12681–12688. [PubMed: 29032680]

(43). Kaur P; Chudasama B Seedless Co-Surfactant-Based Dimensional and Optical Tunability of Gold Nanorods with Simultaneous pH Regulation. J. Mater. Sci 2017, 52, 11675–11687.

(44). Xu D; Mao J; He Y; Yeung ES Size-Tunable Synthesis of High-Quality Gold Nanorods under Basic Conditions by using H_2O_2 as the Reducing Agent. J. Mater. Chem. C 2014, 2, 4989–4996.

(45). Perrault SD; Chan WCW Synthesis and Surface Modification of Highly Monodispersed, Spherical Gold Nanoparticles of 50–200 nm. J. Am. Chem. Soc 2009, 131, 17042–17043. [PubMed: 19891442]

(46). Orendorff CJ; Murphy CJ Quantitation of Metal Content in the Silver-Assisted Growth of Gold Nanorods. J. Phys. Chem. B 2006, 110, 3990–3994. [PubMed: 16509687]

(47). Kozek KA; Kozek KM; Wu W-C; Mishra SR; Tracy JB Large-Scale Synthesis of Gold Nanorods through Continuous Secondary Growth. Chem. Mater 2013, 25, 4537–4544.

(48). Hong H-G; Park W Electrochemical Characteristics of Hydroquinone-Terminated Self-Assembled Monolayers on Gold. Langmuir 2001, 17, 2485–2492.

(49). Walczak MM; Dryer DA; Jacobson DD; Foss MG; Flynn NT Education pH-Dependent Redox Couple: Illustrating the Nernst Equation using Cyclic Voltammetry. J. Chem. Educ 1997, 74, 1195–1197.

(50). Walsh MJ; Tong W; Katz-Boon H; Mulvaney P; Etheridge J; Funston AM A Mechanism for Symmetry Breaking and Shape Control in Single-Crystal Gold Nanorods. Acc. Chem. Res 2017, 50, 2925–2935. [PubMed: 29144733]

(51). Johnson CJ; Dujardin E; Davis SA; Murphy CJ; Mann S Growth and Form of Gold Nanorods Prepared by Seed-Mediated, Surfactant-Directed Synthesis. J. Mater. Chem 2002, 12, 1765–1770.

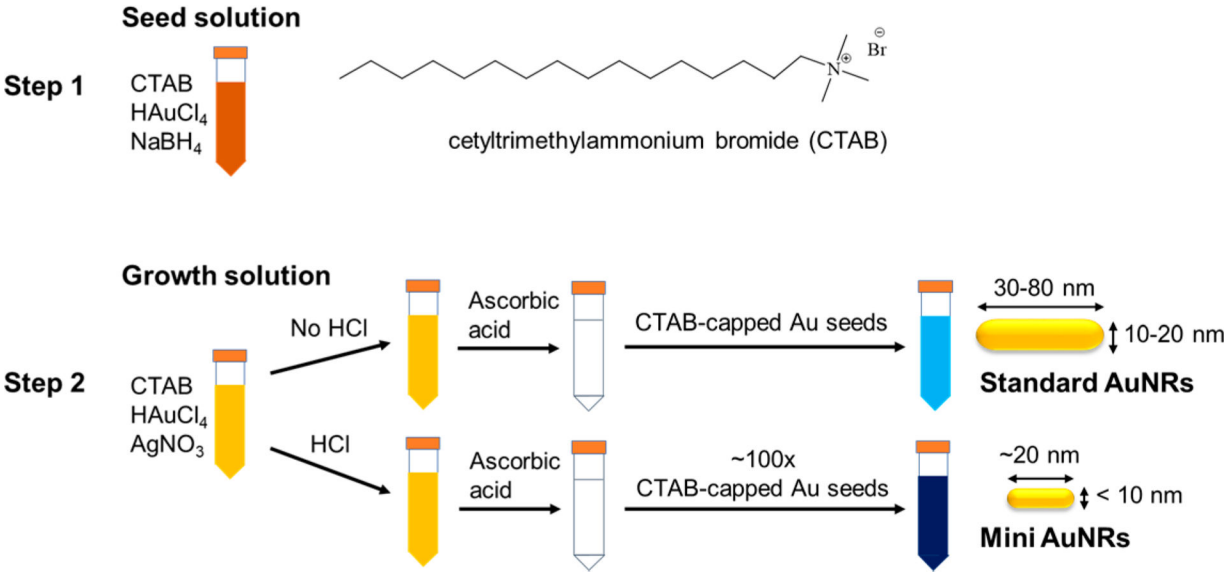

Figure 1.
Schematic representations of major differences between standard and mini AuNR syntheses.

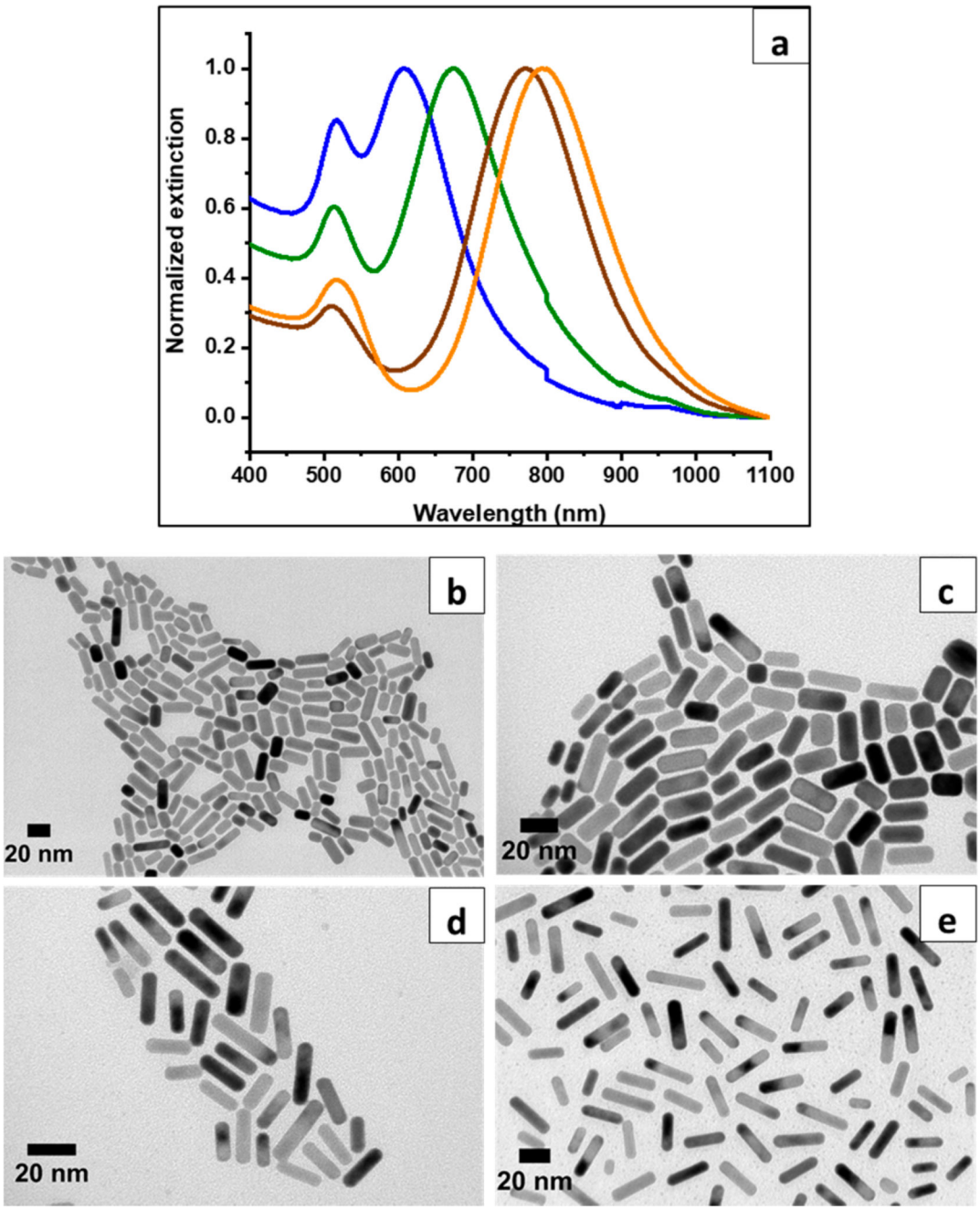

Figure 2.

(a) UV-vis-NIR spectra of mini AuNRs from AR 2.2 to 3.8. The blue, green, brown, and orange spectra correspond to AR 2.2, 2.6, 3.2, and 3.8, respectively. TEM images of ascorbic-acid-reduced mini AuNRs: AR (b) 2.2, (c) 2.6, (d) 3.2, and (e) 3.8.

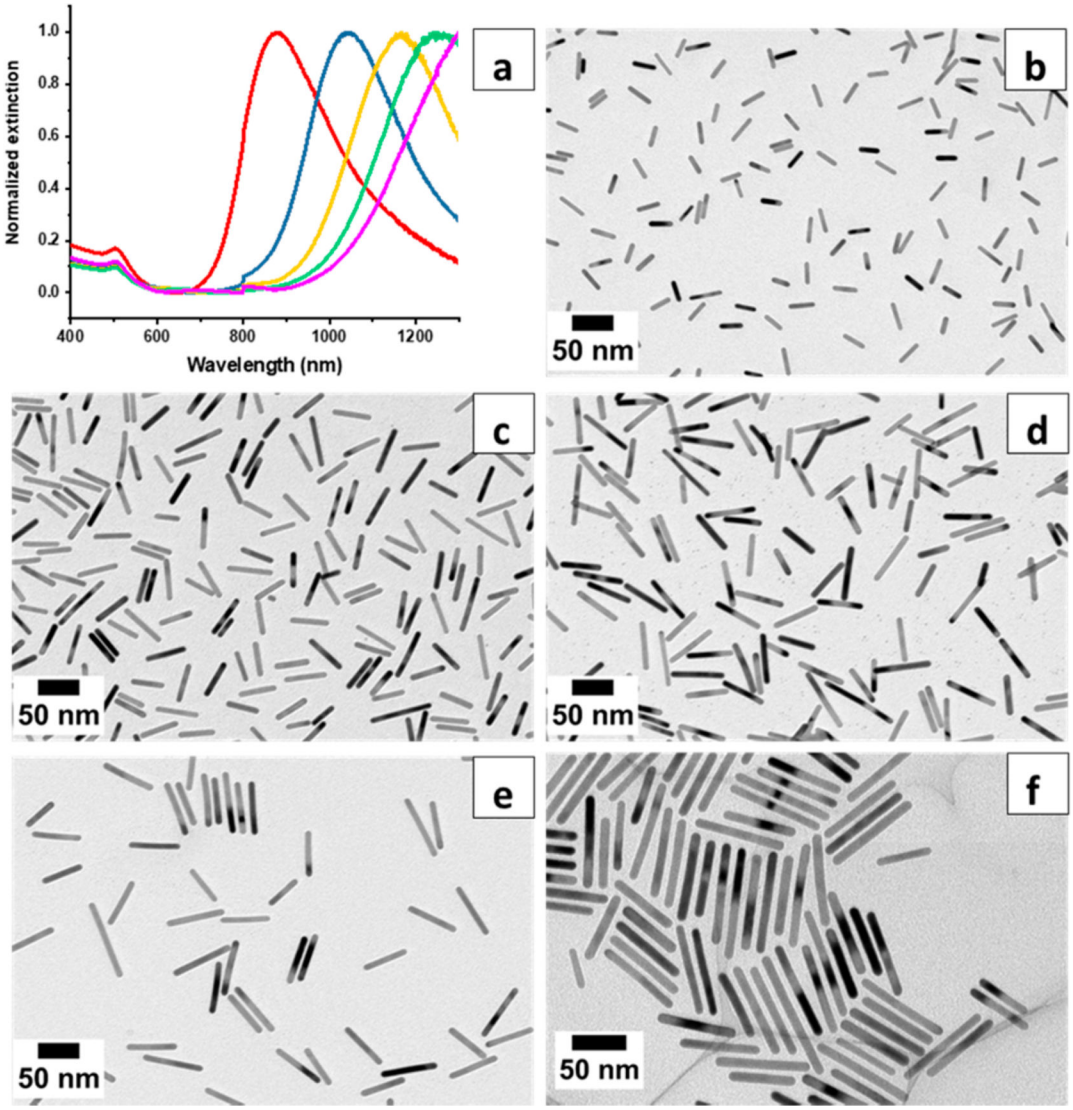

Figure 3.

(a) UV-vis-NIR spectra of mini AuNRs from AR 5.6 (red) to 8.2 (blue), 8.7 (yellow), 9.6 (green), and 10.8 (pink). TEM images of hydroquinone-reduced mini AuNRs, AR (b) 5.6, (c) 8.2, (d) 8.7, (e) 9.6, and (f) 10.8.

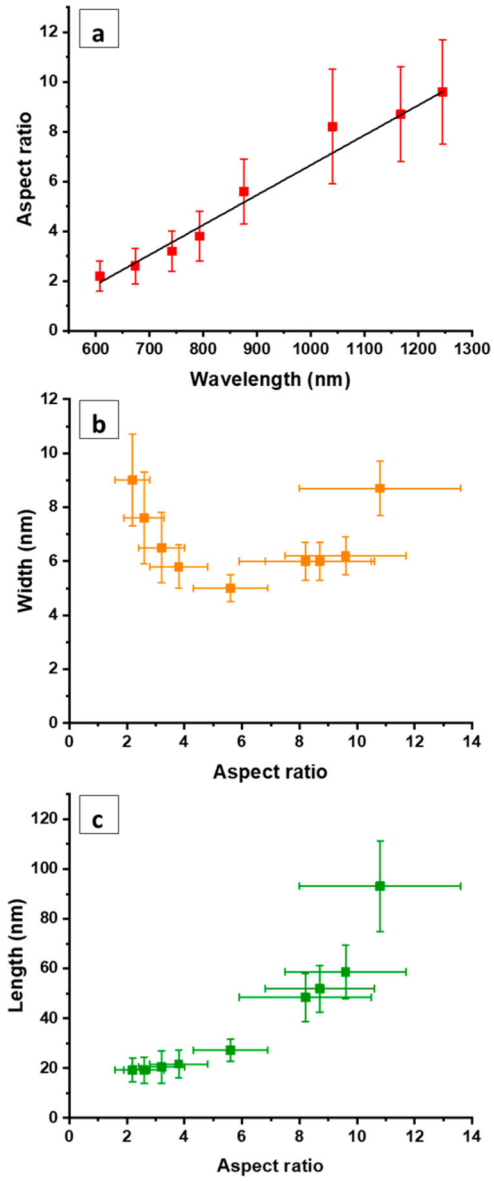

Figure 4.

(a) Linear relationship between the ARs of mini AuNRs and the corresponding longitudinal plasmon band wavelengths; R^2= 0.969 84. Plots of (b) minirod widths versus AR and (c) minirod lengths versus AR, for AR 2.2–10.8.

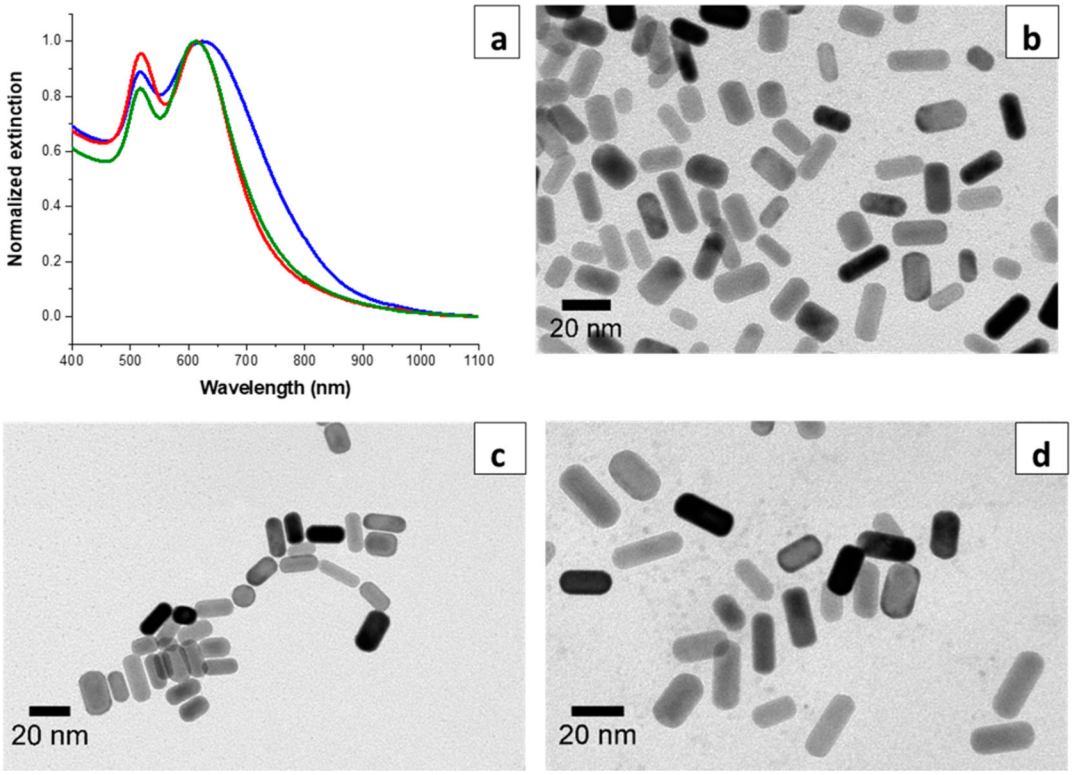

Figure 5.
(a) UV-vis-NIR spectra of mini AuNRs from three 1 L batches. (b-d) TEM images of ascorbic-acid-reduced mini AuNRs of 1 L batches.

Table 1.

Aspect Ratios (ARs), Dimensions, Shape Percent Yield, and Gold Yield of Ascorbic-Acid-Reduced Mini AuNRs[a]

AR	longitudinal LSPR (nm)	length (nm)	width (nm)	shape percent yield (%)	yield (96)
2.2 ± 0.6	607	19.3 ± 4.8	9.0 ± 1.7	96.7 (N = 514)	79
2.6 ± 0.7	673	19.2 ± 5.3	7.6 ± 1.7	96.1 (N = 672)	81
3.2 ± 0.8	771	20.5 ± 6.5	6.5 ± 1.3	89.6 (N = 824)	89
3.8 ± 1.0	793	21.7 ± 5.5	5.8 ± 0.8	96.7 (N = 519)	87

[a]The shape percent is defined by $\frac{\text{no. of NRs}}{\text{no. of all shape}} \times 100\%$. N refers to the number of particles measured. Triplicate measurements for metal concentrations were taken by ICP-MS. The standard deviations of the gold concentrations from AuNRs are less than 0.08%. Yield is calculated from ICP-MS data for initial gold concentration in the growth solution compared to gold concentration in aqua-regia-digested metal nanoparticle solutions.

Table 2.

Aspect Ratios (ARs), Dimensions, Shape Percent Yield, and Gold Yield of Hydroquinone-Reduced Mini AuNRs[a]

AR	longitudinal LSPR (nm)	length (nm)	width (nm)	shape percent yield	(%) yield (%)
5.6 ± 1.3	875	27.2 ± 4.4	5.0 ± 0.5	96.4 (*N* = 345)	91
8.2 ± 2.3	1040	48.4 ± 9.6	6.0 ± 0.7	97.0 (*N* = 334)	~100
8.7 ± 1.9	1167	51.9 ± 9.3	6.0 ± 0.7	96.7 (*N* = 428)	~100
9.6 ± 2.1	1245	58.7 ± 10.8	6.2 ± 0.7	98.8 (*N* = 330)	~100
10.8 ± 2.8	>1300	93.1 ± 18.3	8.7 ± 1.0	95.9 (*N* = 362)	~100

[a]The shape percent is defined by $\frac{\text{no. of NRs}}{\text{no. of all shape}} \times 100\%$. *N* refers to the number of particles measured. Triplicate measurements for metal concentrations were taken by ICP-MS. The standard deviations of the gold concentrations from AuNRs are less than 0.08%. Yield is calculated from ICP-MS data for initial gold concentration in the growth solution compared to gold concentration in aqua-regia-digested metal nanoparticle solutions.

Table 3.

Transverse and Longitudinal Extinction Coefficients[a] of Mini AuNRs from AR 2.2 to 10.8

AR	transverse LSPR (nm)	transverse extinction coefficient (M^{-1} cm^{-1})	longitudinal LSPR (nm)	longitudinal extinction coefficient (M^{-1} cm^{-1}
2.2 ± 0.6	523	$3 \pm 1 \times 10^8$	607	$3 \pm 1 \times 10^8$
2.6 ± 0.7	514	$1.1 \pm 0.5 \times 10^8$	673	$1.6 \pm 0.7 \times 10^8$
3.2 ± 0.8	507	$9 \pm 4 \times 10^7$	771	$2 \pm 1 \times 10^8$
3.8 ± 1.0	507	$7 \pm 2 \times 10^7$	793	$2.0 \pm 0.7 \times 10^s$
5.6 ± 1.3	507	$8 \pm 2 \times 10^7$	875	$2.9 \pm 0.6 \times 10^8$
8.2 ± 2.3	504	$1.8 \pm 0.5 \times 10^8$	1040	$9 \pm 2 \times 10^8$
8.7 ± 1.9	504	$1.8 \pm 0.5 \times 10^8$	1167	$1.0 \pm 0.3 \times 10^9$
9.6 ± 2.1	504	$2.4 \pm 0.6 \times 10^8$	1245	$1.4 \pm 0.3 \times 10^9$
10.8 ± 2.8	504	$7 \pm 2 \times 10^8$	>1300	N/A[b]

[a] Extinction coefficients are reported on a per-particle basis and include the standard deviations in particle dimensions (which is larger than the standard deviation in metal content).

[b] N/A: not available.

Table 4.

Transverse and Longitudinal LSPR Peaks, ARs, Dimensions, and Shape Percent Yields of Mini AuNRs Made from Three 1 L Growth Solutions[a]

1 L mini AuNRs	transverse LSPR (nm)	longitudinal LSPR (nm)	length (nm)	width (nm)	AR	shape percent yield (%)	final purified mini AuNR concentration (M)
batch 1	517	624	16.9 ± 4.2	7.7 ± 1.5	2.3 ± 0.6	97.3 (N = 409)	1.1×10^{-7}
batch 2	519	614	16.2 ± 4.3	8.2 ± 2.1	2.0 ± 0.5	97.2 (N = 322)	7.1×10^{-8}
batch 3	517	613	20.5 ± 5.1	9.6 ± 2.2	2.2 ± 0.6	97.5 (N = 325)	1.5×10^{-7}
average			17.9 ± 4.6	8.5 ± 2.0	2.2 ± 0.6	97.4 (N = 1056)	1.1×10^{-7}

[a]The shape percent yield is defined by $\frac{\text{no. of rods}}{\text{no. of all shape}} \times 100\%$. N refers to the number of particles measured. The 1 L mini AuNR concentrations are calculated based on the extinction coefficients from Table 3.